Transitions in synchronization states of model cilia through basal-connection coupling Supplementary Information

Yujie Liu[1], Rory Claydon[2], Marco Polin[2,3†], and Douglas R. Brumley[1*]
[1] *School of Mathematics and Statistics, The University of Melbourne, Victoria 3010, Australia.*
[2] *Physics Department, University of Warwick, Gibbet Hill Road, Coventry CV4 7AL, UK.*
[3] *Centre for Mechanochemical Cell Biology, University of Warwick, Gibbet Hill Road, Coventry CV4 7AL, UK.*

S1. DERIVATION OF GOVERNING EQUATIONS

In this section we derive the full equations of motion for arbitrary R_0/l. The rotors on the left and right hand side of Fig. 1a are referred to as 1 and 2 respectively. We use the centre of the circular orbit of rotor 1 as the origin of reference. The polar unit vectors for external and internal rotors (1 and 2) are given by

$$\begin{aligned}\mathbf{e}_{r_{1,2}} &= (\cos\phi_{1,2}, \sin\phi_{1,2}),\\ \mathbf{e}_{\phi_{1,2}} &= (-\sin\phi_{1,2}, \cos\phi_{1,2}),\\ \mathbf{w}_{r_{1,2}} &= (\cos(\phi_{1,2}\pm\theta), \sin(\phi_{1,2}\pm\theta)),\\ \mathbf{w}_{\phi_{1,2}} &= (-\sin(\phi_{1,2}\pm\theta), \cos(\phi_{1,2}\pm\theta)).\end{aligned} \tag{S1}$$

The equations for rotor 1 will be derived explicitly, and the corresponding equations for rotor 2 obtained by symmetry. The two internal rotors (see Fig. 1a) are connected by an anisotropic spring of stiffness (k_x, k_y) and equilibrium length $(l, 0)$. The force exerted by internal rotor 2 on internal rotor 1 through this spring is

$$\begin{aligned}f_x &= k_x s(\cos(\phi_2-\theta) - \cos(\phi_1+\theta)),\\ f_y &= k_y s(\sin(\phi_2-\theta) - \sin(\phi_1+\theta)).\end{aligned} \tag{S2}$$

In polar coordinates, we are only interested in the tangential force as the there is no radial freedom for the internal rotors in the model.

$$f_{\phi_1} = (\mathbf{w}_{\phi_1}\cdot\mathbf{e}_x)f_x + (\mathbf{w}_{\phi_1}\cdot\mathbf{e}_y)f_y = -f_x\sin(\phi_1+\theta) + f_y\cos(\phi_1+\theta). \tag{S3}$$

Substituting Eq. (S2) into Eq. (S3) yields

$$f_{\phi_1} = (k_x+k_y)s\big[G(\phi_1+\theta, \phi_2-\theta) - G(\phi_1+\theta, \phi_1+\theta)\big], \tag{S4}$$

where for angles a and b,

$$G(a,b) = \frac{1}{2}\frac{k_y-k_x}{k_x+k_y}\sin(a+b) - \frac{1}{2}\sin(a-b). \tag{S5}$$

To obtain the governing equations of the system, the following assumptions are made:

1. The torque of the system is balanced.

2. The radial force of the system is balanced for each rotor.

This essentially assumes that the system can respond to the external force instantaneously and reach the equilibrium. The motion of the external rotors create hydrodynamic disturbances which are modelled as Stokeslets in an unbounded fluid [1]. To express the Stokeslet flow field produced by external rotor 2, but located at external rotor 1, we define

* d.brumley@unimelb.edu.au, † m.polin@warwick.ac.uk

the effective Stokeslet strength $\mathbf{f}$, which is proportional to the velocity of external rotor 2. The relative positions of the external rotors is given by $\mathbf{r}_{12} = \mathbf{r}_1 - \mathbf{r}_2$.

$$\begin{aligned}
\mathbf{f} &= \frac{3a}{4} R_2 \dot{\phi}_2 \mathbf{e}_{\phi_2} + \frac{3a}{4} \dot{R}_2 \mathbf{e}_{r_2} \\
&= (-l + R_1 \cos\phi_1 - R_2 \cos\phi_2)\mathbf{e}_x + (R_1 \sin\phi_1 - R_2 \sin\phi_2)\mathbf{e}_y. \\
\frac{4}{3a}\mathbf{f} \cdot \mathbf{r}_{12} &= l(R_2\dot{\phi}_2 \sin\phi_2 - \dot{R}_2 \cos\phi_2) + R_1 \dot{R}_2 \cos(\phi_1 - \phi_2) + R_1 R_2 \dot{\phi}_2 \sin(\phi_1 - \phi_2) - R_2 \dot{R}_2. \\
r_{12}^2 &= l^2 - 2l(R_1 \cos\phi_1 - R_2 \cos\phi_2) + R_1^2 + R_2^2 - 2R_1 R_2 \cos(\phi_1 - \phi_2).
\end{aligned} \tag{S6}$$

(1) **Torque Balance**

The torque balance for the overdamped rotor 1 system is similar to [1], but with an additional term. The internal driving force from the flagellar motors is $\mathbf{F}_{\text{int}}^{(1,2)} = \zeta R_0 \omega_{1,2}$.

$$R_1 \dot{\phi}_1 - \mathbf{e}_{\phi_1} \cdot \left(\frac{\mathbf{f}}{r_{12}} + \frac{\mathbf{r}_{12}(\mathbf{f} \cdot \mathbf{r}_{12})}{r_{12}^3} \right) = R_0 \omega_1 + \frac{s f_{\phi_1}}{\zeta R_1}. \tag{S7}$$

The LHS of Eq. (S7) can be expanded using Eq. (S6) to obtain

$$R_1 \dot{\phi}_1 - \frac{3a}{4r_{12}} \left[\frac{M_{12}^+ A_{12}^+}{r_{12}^2} + R_2 \cos(\phi_1 - \phi_2) \right] \dot{\phi}_2 - \frac{3a}{4r_{12}} \left[\frac{M_{12}^+ B_{12}^+}{r_{12}^2} + \sin(\phi_2 - \phi_1) \right] \dot{R}_2. \tag{S8}$$

The equations for rotor 2 can be obtained by swapping the labels (1 and 2) and changing the sign of l. Here we make use of the translational invariance property of the system. This is equivalent to translating the whole system horizontally by l such that the orbit centre of rotor 2 coincides with the origin of the reference frame

$$R_2 \dot{\phi}_2 - \frac{3a}{4r_{12}} \left[\frac{M_{21}^- A_{21}^-}{r_{12}^2} + R_1 \cos(\phi_2 - \phi_1) \right] \dot{\phi}_1 - \frac{3a}{4r_{12}} \left[\frac{M_{21}^- B_{21}^-}{r_{12}^2} + \sin(\phi_1 - \phi_2) \right] \dot{R}_1, \tag{S9}$$

where

$$\begin{aligned}
M_{ij}^{\pm} &= \pm l \sin\phi_i + R_j \sin(\phi_i - \phi_j), \\
A_{ij}^{\pm} &= \pm l R_j \sin\phi_j + R_i R_j \sin(\phi_i - \phi_j), \\
B_{ij}^{\pm} &= \mp l \cos\phi_j + R_i \cos(\phi_i - \phi_j) - R_j.
\end{aligned} \tag{S10}$$

(2) **Radial Force Balance**

Similarly, with the external spring of stiffness λ, the radial force balance is given by the expression

$$\dot{R}_1 - \mathbf{e}_{r_1} \cdot \left(\frac{\mathbf{f}}{r_{12}} + \frac{\mathbf{r}_{12}(\mathbf{f} \cdot \mathbf{r}_{12})}{r_{12}^3} \right) = -\frac{\lambda}{\zeta}(R_1 - R_0). \tag{S11}$$

Although the internal rotors contribute indirectly, the above equation does not involve an explicit contribution from their motion. Using Eq. (S6) we can expand the LHS of Eq. (S11)

$$\dot{R}_1 - \frac{3a}{4r_{12}} \left[\frac{N_{12}^+ A_{12}^+}{r_{12}^2} + R_2 \sin(\phi_1 - \phi_2) \right] \dot{\phi}_2 - \frac{3a}{4r_{12}} \left[\frac{N_{12}^+ B_{12}^+}{r_{12}^2} + \cos(\phi_1 - \phi_2) \right] \dot{R}_2. \tag{S12}$$

By the same symmetry argument, we obtain the radial equation for rotor 2

$$\dot{R}_2 - \frac{3a}{4r_{12}} \left[\frac{N_{21}^- A_{21}^-}{r_{12}^2} + R_1 \sin(\phi_2 - \phi_1) \right] \dot{\phi}_1 - \frac{3a}{4r_{12}} \left[\frac{N_{21}^- B_{21}^-}{r_{12}^2} + \cos(\phi_2 - \phi_1) \right] \dot{R}_1, \tag{S13}$$

where

$$N_{ij}^{\pm} = \mp l \cos\phi_i + R_i - R_j \cos(\phi_i - \phi_j). \tag{S14}$$

From Eqs. (S8)-(S9) and Eqs. (S12)-(S13), the governing equations are therefore

$$\begin{aligned}
&R_1\dot{\phi}_1 - \frac{3a}{4r_{12}}\left[\frac{M_{12}^+A_{12}^+}{r_{12}^2} + R_2\cos(\phi_1-\phi_2)\right]\dot{\phi}_2 - \frac{3a}{4r_{12}}\left[\frac{M_{12}^+B_{12}^+}{r_{12}^2} + \sin(\phi_2-\phi_1)\right]\dot{R}_2 = R_0\omega_1 + \frac{sf_{\phi_1}}{\zeta R_1},\\
&R_2\dot{\phi}_2 - \frac{3a}{4r_{12}}\left[\frac{M_{21}^-A_{21}^-}{r_{12}^2} + R_1\cos(\phi_2-\phi_1)\right]\dot{\phi}_1 - \frac{3a}{4r_{12}}\left[\frac{M_{21}^-B_{21}^-}{r_{12}^2} + \sin(\phi_1-\phi_2)\right]\dot{R}_1 = R_0\omega_2 + \frac{sf_{\phi_2}}{\zeta R_2},\\
&\dot{R}_1 - \frac{3a}{4r_{12}}\left[\frac{N_{12}^+A_{12}^+}{r_{12}^2} + R_2\sin(\phi_1-\phi_2)\right]\dot{\phi}_2 - \frac{3a}{4r_{12}}\left[\frac{N_{12}^+B_{12}^+}{r_{12}^2} + \cos(\phi_1-\phi_2)\right]\dot{R}_2 = -\frac{\lambda}{\zeta}(R_1-R_0),\\
&\dot{R}_2 - \frac{3a}{4r_{12}}\left[\frac{N_{21}^-A_{21}^-}{r_{12}^2} + R_1\sin(\phi_2-\phi_1)\right]\dot{\phi}_1 - \frac{3a}{4r_{12}}\left[\frac{N_{21}^-B_{21}^-}{r_{12}^2} + \cos(\phi_2-\phi_1)\right]\dot{R}_1 = -\frac{\lambda}{\zeta}(R_2-R_0),
\end{aligned} \tag{S15}$$

where f_{ϕ_2} is f_{ϕ_1} in Eq. (S4) but with the exchange $\phi_1 + \theta \leftrightarrow \phi_2 - \theta$.

The set of governing equations is non-linear, and it is useful to simplify the system while preserving some of its important features. One way is to take the small hydrodynamic limit of Eq. (S15), i.e. as $l \gg R_0$, ignore $O(R_{1,2}/l)$. Under this assumption, we obtain Eq. (1) in the paper. If the timescale for changes in $\sigma = \phi_1 + \phi_2$ is long compared to the timescale for $\delta = \phi_1 - \phi_2$ (as is the case in section III), the leading order equation (Eq. (5)) for the phase sum σ can be obtained by summing the leading order contributions from each term in the equations for ϕ_1 and ϕ_2. This gives the hydrodynamic interaction term in [1] plus the leading order term from the anisotropic spring interaction, and is shown in Eq. (4) of the main paper.

This model has the advantage that it can be easily generalized so that the internal basal coupling involves both the phase and amplitude of the external rotors. One possible way is to enable radial freedom to the internal rotors, which can be coupled with the amplitude of the external oscillators via a larger spring that connects the two rotors. However, it can be shown that under the assumptions that (i) the internal spring constant is stiff compared to the sum of external and large spring constants, and (ii) the internal rotor radius is small compared to the external rotor radius, this internal radial freedom does not contribute to the leading order dynamics in Eq. (5).

S2. DERIVATION OF NEXT ORDER GEOMETRIC HIGHER ORDER TERM

In this section, we present the derivation of next-to-leading order term in R_0/l in Eqs. (6)-(7). We aim at geometric higher order terms ($O(R/l)$) in the radial equation for R_1 in Eq. (S15). The case for R_2 can be obtained by symmetry. Since we are interested in the leading order DC component of R_1 at equilibrium, we can drop the term proportional to $\dot{R}$, in which, by taking derivative, the DC component becomes zero and the oscillatory components remain. Thus the radial equation simplifies to

$$-\frac{3a}{4r_{12}}\left[\frac{N_{12}^+A_{12}^+}{r_{12}^2} + R_2\sin(\phi_1-\phi_2)\right]\dot{\phi}_2 = -\frac{\lambda}{\zeta}(R_1-R_0). \tag{S16}$$

From section S1, recall the definitions for r_{12}, $A_{ij}^{\pm}$, $N_{ij}^{\pm}$ in Eq. (S6), (S10) and (S14). We set $R_1 = R_2 = R_0$ in those expressions by taking the leading order DC component of radius (assume the radius R_1 is dominated by R_0 and next order is small), then they become

$$\begin{aligned}
r_{12}^2 &= l^2 - 2lR_0(\cos\phi_1 - \cos\phi_2) + 2R_0^2(1-\cos\delta),\\
A_{12}^+ &= lR_0\sin\phi_2 + R_0^2\sin\delta,\\
N_{12}^+ &= -l\cos\phi_1 + R_0(1-\cos\delta).
\end{aligned} \tag{S17}$$

Expanding $1/r_{12}^3$ and $1/r_{12}$ using Taylor series yields

$$\begin{aligned}\frac{1}{r_{12}^3} &= \frac{1}{l^3}\left[1-\left(\frac{2R_0}{l}(\cos\phi_1-\cos\phi_2)-\frac{2R_0^2}{l^2}(1-\cos\delta)\right)\right]^{-\frac{3}{2}}\\ &= \frac{1}{l^3}\left(1+\frac{3R_0}{l}(\cos\phi_1-\cos\phi_2)-\frac{3R_0^2}{l^2}(1-\cos\delta)+\frac{15R_0^2}{2l^2}(\cos\phi_1-\cos\phi_2)^2+O\left(\frac{R_0^3}{l^3}\right)\right),\\ \frac{1}{r_{12}} &= \frac{1}{l}\left[1-\left(\frac{2R_0}{l}(\cos\phi_1-\cos\phi_2)-\frac{2R_0^2}{l^2}(1-\cos\delta)\right)\right]^{-\frac{1}{2}}\\ &= \frac{1}{l}\left(1+\frac{R_0}{l}(\cos\phi_1-\cos\phi_2)-\frac{R_0^2}{l^2}(1-\cos\delta)+\frac{3R_0^2}{2l^2}(\cos\phi_1-\cos\phi_2)^2+O\left(\frac{R_0^3}{l^3}\right)\right).\end{aligned} \tag{S18}$$

The terms of order $O(R^3/l^3)$ in Eq. (S18) are dropped. Next we make note of the following identity for later convenience:

$$(\cos\phi_1-\cos\phi_2)^2 = 1+\cos\sigma(\cos\delta-1)-\cos\delta. \tag{S19}$$

We now consider the terms on the LHS of Eq. (S16) one by one. First we look at the second term, utilising the Taylor expansion in Eq. (S18)

$$R_0\frac{\sin\delta}{r_{12}} \approx \frac{R_0\sin\delta}{l}\left(1+\frac{R_0}{l}(\cos\phi_1-\cos\phi_2)-\frac{R_0^2}{l^2}(1-\cos\delta)+\frac{3R_0^2}{2l^2}(\cos\phi_1-\cos\phi_2)^2\right). \tag{S20}$$

From here on we use the fact that when the intrinsic frequencies ω_1 and ω_2 are dominating the dynamics, they have similar magnitude but opposite sign (we use $\omega_1 = -\omega_2 = 100\pi$ rad·s^{-1} in this paper), and the rate of change of $\delta \sim 2\omega_1 t$ is much faster than $\sigma \sim 0$. Under the time scale that is large for changes in δ but small for changes in σ, the resulting average of $\sin\delta$, $\cos\delta\sin\delta$, $\sin\delta\cos\phi_{1,2}$ are all zero and we can treat any function of σ as approximately constant. Therefore we have

$$\left\langle R_0\frac{\sin\delta}{r_{12}}\right\rangle \approx 0.$$

We need only focus on the other term on the LHS in Eq. (S16)

$$\begin{aligned}\frac{N_{12}^+A_{12}^+}{r_{12}^3} \approx{}& (-l\cos\phi_1+R_0(1-\cos\delta))(lR_0\sin\phi_2+R_0^2\sin\delta)\\ &\frac{1}{l^3}\left(1+\frac{3R_0}{l}(\cos\phi_1-\cos\phi_2)-\frac{3R_0^2}{l^2}(1-\cos\delta)+\frac{15R_0^2}{2l^2}(\cos\phi_1-\cos\phi_2)^2\right).\end{aligned} \tag{S21}$$

By similar argument above, we may drop the terms multiplied by $\sin\delta$ as they average to 0. So

$$\begin{aligned}\left\langle\frac{N_{12}^+A_{12}^+}{r_{12}^3}\right\rangle \approx{}& \frac{R_0}{l}\sin\phi_2\left(-\cos\phi_1+\frac{R_0}{l}(1-\cos\delta)\right)\\ &\left(1+\frac{3R_0}{l}(\cos\phi_1-\cos\phi_2)-\frac{3R_0^2}{l^2}(1-\cos\delta)+\frac{15R_0^2}{2l^2}(\cos\phi_1-\cos\phi_2)^2\right)\end{aligned} \tag{S22}$$

Multiplying term by term, notice the first term is $-\sin\phi_2\cos\phi_1 = (\sin\delta-\sin\sigma)/2$, as usual we can drop $\sin\delta$ on average. Therefore,

$$\begin{aligned}&\left\langle-\frac{R_0}{2l}\sin\sigma\left(1+\frac{3R_0}{l}(\cos\phi_1-\cos\phi_2)-\frac{3R_0^2}{l^2}(1-\cos\delta)+\frac{15R_0^2}{2l^2}(\cos\phi_1-\cos\phi_2)^2\right)\right\rangle\\ &\approx -\frac{R_0}{2l}\sin\sigma\left(1+\frac{9R_0^2}{2l^2}-\frac{15R_0^2}{2l^2}\cos\sigma\right).\end{aligned} \tag{S23}$$

For the second multiplication, we note that $\sin\phi_2$ oscillates slower than $\cos\delta$ and $\cos^2\delta$ and we always drop $O(R^4/l^4)$. So on average we only need to focus on

$$\begin{aligned}\left\langle\frac{R_0^2}{l^2}\sin\phi_2(1-\cos\delta)\left(\frac{3R_0}{l}(\cos\phi_1-\cos\phi_2)\right)\right\rangle &= \left\langle\frac{3R_0^3}{l^3}(1-\cos\delta)(\sin\sigma-\sin(2\phi_2))/2\right\rangle\\ &= \frac{9R_0^3}{4l^3}\sin\sigma.\end{aligned} \tag{S24}$$

Combining the DC contributions from Eq. (S23) and (S24), we obtain the net contribution

$$-\frac{R_0}{2l}\sin\sigma\left(1-\frac{15R_0^2}{2l^2}\cos\sigma\right). \tag{S25}$$

Substituting this back to Eq. (S16), we have the result for the next-to-leading order in R_0/l for average radial dynamics (take $\dot{\phi}_2 \approx \omega_2$ at leading order)

$$R_1 = R_0 - R_0\frac{\rho\zeta\omega_2}{\lambda}\left(1-\frac{15R_0^2}{2l^2}\cos\sigma\right)\sin\sigma. \tag{S26}$$

The higher order term has a direct impact on the leading order equation Eq. (5). By Taylor expanding the radius at denominator of $\dot{\phi}_{1,2} = R_0\omega_{1,2}/R_{1,2} + \cdots$ and taking the first order correction, we arrive at the modification for σ shown in Eq. (6).

S3. PREDICTION OF ROTOR'S PHASE SPEED

Assume the system ($\theta = 0$ for simplicity) is in equilibrium and both oscillators are beating, hence σ is constant and δ follows

$$\dot{\delta} = A - B\sin\delta, \tag{S27}$$

where $|A| > |B|$. This can be solved by substitution and yields

$$\tan\left(\frac{\delta}{2}\right) = \frac{\Delta\tan u + B}{A}, \tag{S28}$$

where $\Delta = \sqrt{A^2 - B^2}$ and $u = \Delta t/2 + c$ for some constant c. From this, we find that

$$\sin\delta = \frac{\frac{\Delta}{A}\sin(2u) + 2\frac{B}{A}\cos^2 u}{1 + \frac{B^2}{A^2}\cos(2u) + \frac{\Delta B}{A^2}\sin(2u)}. \tag{S29}$$

Integrating Eq. (S29) over a period and taking the time average, we arrive at

$$\langle\sin\delta\rangle = \frac{A - \sqrt{A^2 - B^2}}{B} = \frac{B}{2A} + O\left(\frac{B^3}{A^3}\right). \tag{S30}$$

If we look back to Eq. (3) for σ and δ, we can substitute the corresponding A and B and obtain the leading order phase speed for ϕ_1 (for ϕ_2 it is opposite sign). In either the AP or IP state this is given by

$$\begin{aligned}\langle\dot{\phi}_1\rangle &= \langle\omega_1 - \frac{s^2}{2\zeta R_0^2}\left(k_+\sin\delta + k_-\cos\sigma\sin\delta\right)\rangle \\ &\approx \omega - \frac{\omega}{2}\left(\frac{s^2}{2\zeta\omega R_0^2}\right)^2\left(k_+ + k_-\cos\sigma\right)^2\end{aligned} \tag{S31}$$

where $(k_+, k_-) = (k_y + k_x, k_y - k_x)$. Equation (S31) also suggests the amplitude of instantaneous oscillation of phase speed is given by $|\frac{s^2}{2\zeta R_0^2}\left(k_+ + k_-\cos\sigma\right)|$ and the oscillation always crosses the intrinsic speed ω. The implications of this formula are that in AP ($\sigma = 0$) and IP ($\sigma = \pi$), the phase speed correction is proportional to k_y^2 and k_x^2 respectively. Physically in AP and IP states, the springs in the x and y directions have achieved their equilibrium lengths, and thus do not contribute to the dynamics. Provided k_x (in IP) $> k_y$ (in AP), average phase speed is lower in IP but accompanies a larger oscillation. If k_x is fixed and k_y is changed to achieve transition, the phase speed in the IP state is lower than in the AP state. However, if k_y is fixed and k_x is changing, the situation is reversed.

Equations (S30) and (S31) compare very well with numerical simulations. For $k_x = 0.015$ Nm^{-1}, $k_y = 0.006$ Nm^{-1}, and other parameters as in Table I, the estimate from simulations yields phase speed 42.071 Hz. Equation (S30) predicts 42.071 Hz, and the leading order gives 42.070 Hz. For $k_x = 0.008$ Nm^{-1} and $k_y = 0.015$ Nm^{-1}, simulations predict 34.672 Hz, Eq. (S30) gives 34.672 Hz and the leading order gives 37.022 Hz.

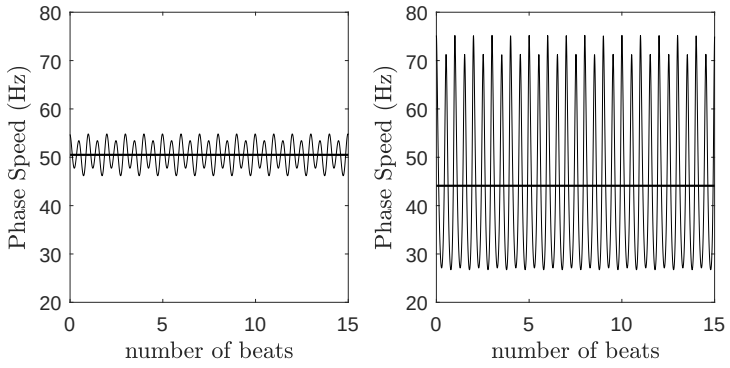

FIG. S1. Instantaneous phase speed profile with hydrodynamics present. Black bold lines indicate the average phase speed. (left) $k_x = 0.005$ Nm^{-1} and $k_y = 0$ Nm^{-1} in AP. (right) $k_x = 0.005$ Nm^{-1} and $k_y = 0.02$ Nm^{-1} in IP.

We can apply similar reasoning to the case in Eq. 1, in which the rotors are also coupled through hydrodynamic interactions. The leading order for δ, analogous to σ, is given by

$$\dot{\delta} = 2\omega + 2\rho\omega\cos\sigma + O\left(\rho\omega\sin\delta\right) + \text{the internal coupling terms for } \delta \text{ in Eq. (3).} \tag{S32}$$

Applying Eq. (S30) using this modified definition for A and B gives the phase speed for ϕ_1 in AP or IP with hydrodynamic interactions present in the limit $R_0 \ll l$:

$$\langle\dot{\phi}_1\rangle \approx \omega + \omega\rho\cos\sigma - \frac{\omega}{2}\left(\frac{s^2}{2\zeta\omega R_0^2}\right)^2 (k_+ + k_-\cos\sigma)^2. \tag{S33}$$

The expression consists of the basal coupling term in Eq. (S31), together with a hydrodynamic correction. This hydrodynamic correction enhances the phase speed for the AP state and reduces it in the IP state, as expected physically [2].

For the physical parameters used in the paper (Table I), the basal coupling term is dominating Eq. (S33) as $\rho \approx 0.02$ is small. If the system is achieving a transition in synchronization states (IP $\leftrightarrow$ AP) through changes in just one of (k_x, k_y), to be consistent with the experimental observation of significant changes in phase speed, the model suggests k_y is the primary variable basal coupling.

In the simulations presented in the paper (with hydrodynamics), where we only vary k_y, we observed the phase speed is lower in the IP state compared to the AP state. For parameters used in Table I and $k_x = 0.005$ Nm^{-1}, the phase speed reduction between $k_y = 0$ Nm^{-1} and $k_y = 0.02$ Nm^{-1} is about 12.7% (see Fig. S1). The formula Eq. (S33) predicts a reduction of about 13.6%.

S4. EXISTENCE OF LARGER EXCURSION MODES

In section IV of the main paper, Fig. 5a,b demonstrates that for intermediate values of k_y, the phase sum $\sigma(t)$ oscillates with large amplitude but zero mean, on a timescale that is long compared to the individual rotor period (see panel (iii)). Figure S2 illustrates the effect of increasing the radius, a, of the model cilium. The chosen value $k_y = 7.65 \times 10^{-3}$ Nm^{-1} is just below the symmetry breaking threshold. For these parameters, the phase sum oscillates between $\approx \pi$ and $-\pi$ with a period of ≈ 12 beats. While $\langle\sigma(t)\rangle = 0$ would suggest an AP state, this system actually spends considerable time close to IP states ($\sigma = \pm\pi$), with rapid swings past the $\sigma = 0$ states.

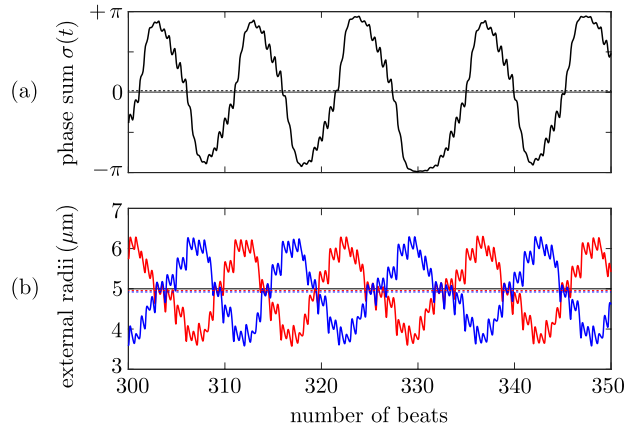

FIG. S2. Deterministic switching between IP and AP states. (a) Phase sum $\sigma(t) = \phi_1(t) + \phi_2(t)$ and (b) external rotor radii, $R_i(t)$. Parameters are as in Table I, except with $a = 1$ μm, $k_x = 5 \times 10^{-3}$ Nm^{-1}, and $k_y = 7.65 \times 10^{-3}$ Nm^{-1}.

S5. COEXISTENCE OF SYNCHRONIZED STATES

Figure 5c,e in the main text shows that for $l \leq 35$ μm, the full system displays a discontinuous transition in $\langle\sigma(t)\rangle$ as k_y is increased. For each of the numerical simulations used to produce Fig. 5c,e, the same initial conditions were used, $(\phi_1, \phi_2) = (0, \pi/2)$. In this section, we further examine the nature of this discontinuity, and explore the capacity for the system to support alternative values of $\langle\sigma(t)\rangle$ for the same (k_x, k_y).

For the *Chlamydomonas*-like separation of $l = 15\,\mu$m, we start with a value of $k_y = 6.5 \times 10^{-3}$ Nm^{-1}, for which $\langle\sigma(t)\rangle$ converges to zero (AP). Once the steady state is achieved, we gradually increase the value of k_y, on a timescale much longer than all other timescales in the system. The system continues to support AP synchronization until $k_y \simeq 6.7 \times 10^{-3}$ Nm^{-1}, at which point a discontinuous jump brings the system to another stable point with $\langle\sigma(t)\rangle = \pm 0.32$ (see Fig. S3). Similarly, starting instead at $k_y = 6.8 \times 10^{-3}$ Nm^{-1} along the positive $\langle\sigma(t)\rangle$ branch, we can gradually decrease the k_y value keeping on the same branch until $k_y \simeq 6.6 \times 10^{-3}$ Nm^{-1}, at which point the average phase sum jumps to $\langle\sigma(t)\rangle = 0$. As Fig. S3 illustrates, there is clearly a small but finite interval in k_y where the system displays 3-state multi-stable dynamics (symmetric negative branch of $\langle\sigma(t)\rangle$ not shown). In this small region, the relative sizes of the basins of attraction for the different states depend on the value of k_y.

The region of parameter space in which this coexistence occurs is relatively small compared to the overall transition zone presented in Fig. 5c (6.6×10^{-3} Nm^{-1} $< k_y <$ 17×10^{-3} Nm^{-1}). Moreover, the width of the coexistence zone diminishes with increasing separation l and eventually disappears for $35\,\mu\text{m} < l < 50\,\mu\text{m}$, when the bifurcation changes nature. As the 3-states coexistence region is narrow, it seems more likely that changes in the synchronization state would be mediated through underlying changes in the basal body stiffness, as outlined in the main text, rather than stochastic jumping between the coexisting states for a fixed k_y.

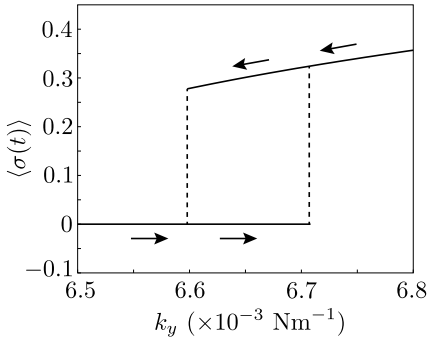

FIG. S3. Bifurcation diagram showing $\langle\sigma(t)\rangle$ as a function of k_y, for $l = 15$ μm and $k_x = 5 \times 10^{-3}$ Nm^{-1}. Symmetric negative $\langle\sigma(t)\rangle$ branch not shown. All other parameters are as in Table I.

[1] Niedermayer T, Eckhardt B, Lenz P. 2008 Synchronization, phase locking, and metachronal wave formation in ciliary chains. *Chaos* **18**, 037128. (doi:10.1063/1.2956984)

[2] Leptos KC, Wan KY, Polin M, Tuval I, Pesci AI, Goldstein RE. 2013 Antiphase synchronization in a flagellar-dominance mutant of *Chlamydomonas*. *Phys. Rev. Lett.* **111**, 158101. (doi:10.1103/PhysRevLett.111.158101)